Chemistry & Biology, Vol. 10, 1233–1243, December, 2003, ©2003 Elsevier Science Ltd. All rights reserved. DOI 10.1016/j.chembiol.2003.11.015

Generalized RNA-Directed Recombination of RNA

Craig A. Riley and Niles Lehman*
Department of Chemistry
Portland State University
P.O. Box 751
Portland, Oregon 97207

Summary

RNA strand exchange through phosphor-nucleotidyl transfer reactions is an intrinsic chemistry promoted by group I intron ribozymes. We show here that *Tetrahymena* and *Azoarcus* ribozymes can promote RNA oligonucleotide recombination in either two-pot or one-pot schemes. These ribozymes bind one oligonucleotide, cleave following a guide sequence, transfer the 3′ portion of the oligo to their own 3′ end, bind a second oligo, and catalyze another transfer reaction to generate recombinant oligos. Recombination is most effective with the *Azoarcus* ribozyme in a single reaction vessel in which over 75% of the second oligo can be rapidly converted to recombinant product. The *Azoarcus* ribozyme can also create a new functional RNA, a hammerhead ribozyme, which can be constructed via recombination and then immediately promote its own catalysis in a homogeneous milieu, mimicking events in a prebiotic soup.

Introduction

Recombination is the swapping of genetic information between two sources. It is a fundamental biological process critical to the production of biological diversity, to the maintenance of high-fitness genotypes, and to the repair of damaged genetic material. In contemporary organisms, recombination usually involves the alignment of multiple strands of DNA with similar sequences, and it requires a protein enzyme to catalyze strand swapping, strand breakage, and strand religation. In *E. coli*, for example, the RecA protein and many associated enzymes are responsible for homologous recombination of DNA [1]. The resulting, or recombinant, strands possess one of many possible mosaic sequences of the original, or parental, strands.

Recombination of RNA strands is also possible and is today observed in RNA viruses where template jumping of viral RNA replicases engenders crossing-over events [2]. In fact, RNA recombination may have been a central feature of the RNA world and thus involved in the origins of life [3–7]. Gilbert speculated that the first stage of evolution proceeded by RNA molecules evolving "in self-replicating patterns, using recombination and mutation to explore new functions and to adapt to new niches" [3], and Cech noted that "if the earliest genes were made of RNA, then RNA splicing can be considered to be the first form of genetic recombination" [4]. These sentiments were doubtless inspired by the reactions catalyzed by the *Tetrahymena thermophila* ribozyme, one of the first examples of RNA-directed catalysis discovered. The *Tetrahymena* ribozyme is an example of group I introns (Figure 1), which catalyze their own self-splicing in vivo via a two-step transesterification reaction [8, 9]. The transesterifications occur with a ΔG near zero and result in the displacement of a RNA phosphoester bond from one dinucleotide site to another. Consequently, the group I reaction pathway bears a strong similarity to contemporary recombination in which DNA phosphoester bonds are swapped at least once between two parental strands.

The potential for catalytic RNA to promote recombinase-like activity was first hinted at when it was shown that the *Tetrahymena* ribozyme could degrade a homogeneous population of pC_5 (pentacytidine 5′-phosphate) into a continuum of products ranging from 3 to 30 nucleotides in length [9]. It was subsequently observed that this ribozyme could bind a wide range of oligoribonucleotides and catalyze phosphoester transfer reactions that mimic either the forward or reverse reactions of self-splicing [10], leading to the demonstration that it could potentially repair defective mRNA sequences by effectively ligating 5′ and 3′ exons from two different sources [11]. In this latter case, a shortened form of the ribozyme, termed L-21 because the first 21 nucleotides of the wild-type intron have been removed such that the first six nucleotides constitute the internal guide sequence (IGS), can be prepared with the "repair" 3′ exon attached to the 3′ end of the ribozyme. This construct can then bind an exogenous substrate consisting of a "truncated" 5′ exon followed by the 6-nt recognition sequence complementary to the IGS and catalyze a phosphoester transfer reaction that liberates the ligated, and hence repaired, exons [11]. Such an approach has been utilized in the repair of defective transcripts of various genes, such as sickle β-globin [12], p53 [13], and others. In addition, group I ribozymes can be engineered to perform a *trans* excision-splicing reaction in which intervening sequences of exogenous RNA substrates are spliced out [14]. Similarly, an engineered twin-hairpin ribozyme has recently been shown to excise and repair a mismatched RNA region in a particular RNA substrate [15].

These repair strategies involve elements of recombination, but they are not generalized because at least one of the parental strands is initially covalently bound to the ribozyme, and the ribozyme is restricted from performing multiple turnover and behaving as a recombinase. However, the 1044-nt lariat bI1 intron of the yeast group II ribozyme and its 786-nt linear form have previously been shown to exhibit a small amount of recombinase-like activity on one pair of large (250–625 nt) substrate RNAs [16]. Recombination in this system was achieved by the sequential binding of two distinct substrates that possess in common only the 6-nt intron binding site (IBS; the group II equivalent of the IGS for group I introns), and the resulting swapping of the head

*Correspondence: niles@pdx.edu

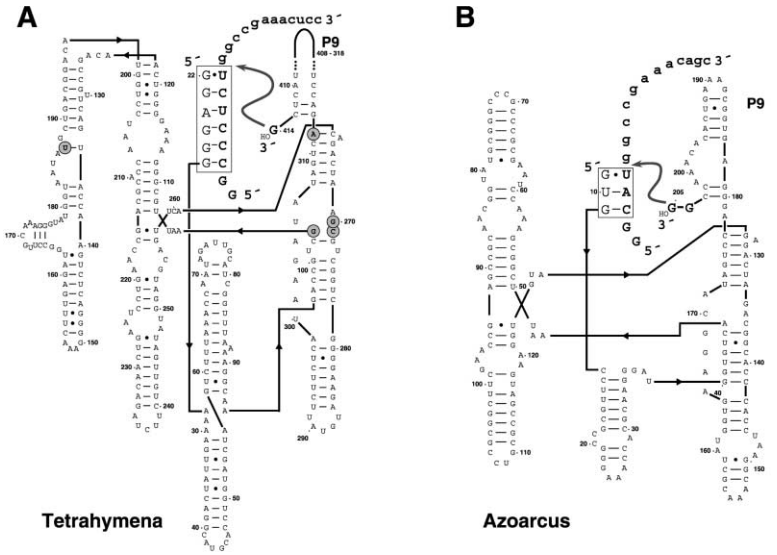

Figure 1. The Primary Sequences and Secondary Structures of the Group I Ribozymes Used in This Study as Recombinases

The group I ribozymes used in this study as recombinases. Primary sequences and secondary strucutres are from previous studies [21, 30]. The internal guide sequence IGS is boxed; the exogenous substrate is depicted in boldface type with lowercase letters denoting nucleotides in the "tail" portion that becomes transiently attached to the 3′ end of the ribozyme following transesterification promoted by nucleophilic attack (arrow) by the terminal G residue on the splice site.

(A) The L-21 *Tetrahymena* 5-error variant that exhibits slowed tail hydrolysis [24], particularly in buffers containing Ca^{2+}. Mutations from the wild-type sequence are indicated in shaded circles: $A_{103}\rightarrow G$, $A_{187}\rightarrow U$, $A_{270}\rightarrow G$, $U_{271}\rightarrow C$, $G_{312}\rightarrow A$. Substrate shown bound is S-3t; nucleotides in P9 stems are omitted for clarity.

(B) The L-8 *Azoarcus* variant derived from the L-10 construct [21] of the wild-type sequence [20]. The two terminal G residues were returned to the L-10 variant via the PCR. Substrate shown bound is S-3a.

of one substrate with the tail of the other and vice versa [16]. Later, an indication that group I ribozymes might be suitable as recombinases came when the $tRNA^{Ile}$ intron from the purple bacterium *Azoarcus* was shown to be able to polymerize short 3′ exons by sequential transesterification reactions [17] and that this process could be altered to generate, in one instance, a polymer of heterogeneous monomeric units [18].

Motivated by the above findings, we endeavored to exploit the transesterification reaction potential of group I introns to demonstrate, optimize, and generalize the recombinase activities of this class of ribozymes. We reasoned that by the use of shortened forms of group I introns with endogenous 3′ guanosines to provide the nucleophile for transesterification, a two-stage reaction could take place in vitro that invokes the reverse of the second step of in vivo splicing followed by the forward of the first step of in vivo splicing (Figure 2). In the first stage, the free ribozyme would bind one exogenous substrate (**A•B**, where the dot indicates the splice site) via complementary base pairing at the IGS, promote cleavage at the splice site, and transfer the 3′ portion of the substrate to the 3′ end of the ribozyme. This "pick-up-the-tail" (PUTT) reaction is well characterized [9] and can be used as a fulcrum to select ribozymes with desired activities out of randomized pools (e.g., [19]). In the second stage, if the 3′ end of the first substrate diffuses out of the catalytic pocket or can be competitively displaced by a second (**C•D**) substrate, then the ribozyme should be able to promote the nucleophilic attack of either endogenous or exogenous guanosine on the **C•D** substrate, thereby catalyzing recombination (REC) and creating the recombinant **C•B** product. Conversely, the reciprocal events could be catalyzed, such that the overall reaction (i.e., cross) would be:

$$\mathbf{A{\bullet}B} \times \mathbf{C{\bullet}D} \rightleftarrows \mathbf{C{\bullet}B} + \mathbf{A{\bullet}D}. \qquad (1)$$

The position of the equilibrium should be affected by relative substrate concentrations, while the kinetics of the reaction should be determined by K_m values between the ribozyme and the various substrates, the k_{cat} values for transesterification, and the K_d and rate constants for competing side reactions. In particular, free-intron constructs of group I ribozymes have varying tendencies to lose their 3′ tails following the PUTT reaction via general base-catalyzed site-specific hydrolysis at the 3′ splice site. Other major constraints on the reaction include the necessity for the head portions of the substrates to possess IGS-complement sequences and the potential for secondary structure in the substrates to interfere with binding to the ribozyme.

In this report, we explore the recombinase potential of shortened forms of both the rRNA intron from the ciliate *Tetrahymena* and the $tRNA^{Ile}$ intron from the phylogenetically distant bacterium *Azoarcus* BHZ23 [20, 21]. For the former, we focused on a five-error variant of the wild-type L-21 molecule that exhibits a reduced rate of spontaneous tail hydrolysis. The latter is distinct in its small size (195 nt), its high G + C content (71%), its high temperature optimum (60°C), and its IGS, which can be shortened in vitro to as little as the trinucleotide GUG. To the truncated versions of both of these molecules we added an endogenous G nucleophile to their 3′ ends, such that they could participate in the recombination scheme outlined in Figure 2. We found that both ribozymes are remarkably adept at promoting recombination between short RNA oligonucleotide substrates, catalyzing transient recombination frequencies (*RF*s) as high as 78% in a single reaction vessel. Furthermore, we were able to demonstrate how such recombination could result in the buildup of genetic information through the creation of other catalytic RNAs. These findings have direct bearing on the potential role of recombination

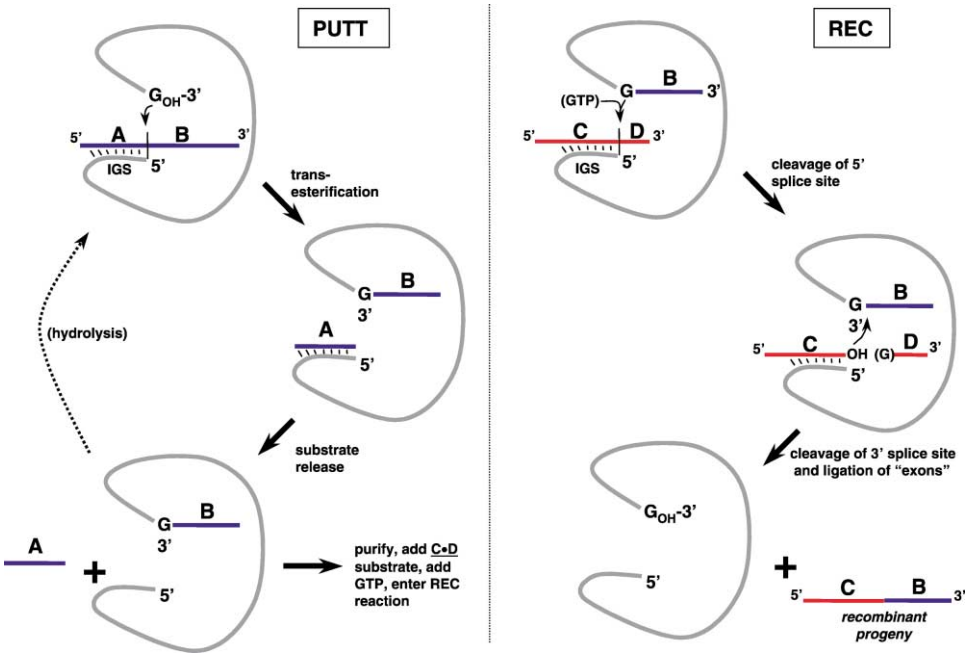

Figure 2. Two-Pot Recombination Scheme Based on the Transesterification Reactions Catalyzed by Group I Introns

In the first reaction (left panel), the ribozyme is incubated with an excess of oligoribonulceotide substrate **A•B** for 1–2 hr at its optimal reaction temperature in 50 mM $MgCl_2$. The transesterification that results is the equivalent of the reverse of the second step of splicing in vivo, in which the 3′ portion of the substrate is covalently attached to the 3′ end of the ribozyme in a "pick-up-the-tail" (PUTT) reaction. Following incubation, the ribozyme is purified from remaining unreacted substrate and buffer by size-selected spin column application (e.g., Nanosep 30K). In the second reaction (right panel), the tailed ribozyme is incubated in excess over oligoribonulceotide substrate **C•D** for 1–2 hr at its optimal reaction temperature in 50 mM $MgCl_2$. The transesterification that results is the equivalent of the forward of the first step of splicing in vivo and results in the recombination (REC) of the substrates such that the recombinant product **C•B** is produced. If the **C•D** substrate is radioactively tagged on the 5′, or "head," portion, then the recombination can be easily observed by gel electrophoresis (Figure 3). During REC, exogenous GTP can be added with only a marginal improvement on recombination frequencies (*RF*, defined as percentage of **C•D** converted to **C•B**), which range from 5%–45%, depending on ribozymes, substrates, and reaction conditions.

in the RNA world and expand yet again the catalytic repertoire of RNA.

Results and Discussion

Two-Pot Recombination

As a starting point, we assayed the ability of group I introns to create recombinant oligonucleotide products in a two-step process, PUTT + REC, each occurring in a separate reaction vessel. We designed a series of RNA oligonucleotides that would allow us to detect RNA-directed recombination (Table 1). Each oligo has a 5′ "head" region containing the IGS complement, and a 3′ "tail" region downstream of the splice site (i.e., **A•B**). When in vitro constructs of the group I ribozyme containing a endogenous 3′ G nucleophile are incubated with such substrates in a *trans*-splicing format, cleavage occurs at the splice site and the tail is transferred to the 3′ end of the ribozyme (PUTT) via transesterification. When a new substrate **C•D** becomes available such that the stoichiometry favors a second transesterification event involving the new substrate, the REC reaction should generate recombinant oligos in which the head of one is recombined with the tail of another (**C•B**, Figure 2).

We first tested this scheme on the *Tetrahymena* L-21 ribozyme (Figure 3). To skew the stoichiometry to promote recombination, we used two strategies. First, we incubated 10 pmol of ribozyme with 25 pmol of **A•B** in the PUTT reaction, but with only 1 pmol of **C•D** in the REC reaction. These ratios favor the conversion of ribozymes to tailed ribozymes initially, then favor the conversion of **C•D** oligos into recombinant **C•B** oligos. Second, we separated tailed ribozymes away from unreacted substrates following the PUTT reaction with a Nanosep 30K column, which partition based on a molecular-weight cut-off of 30–60 kDa. Thus, there should be little if any competition of **C•D** oligos with cleaved **A** heads in the REC reaction for binding to the IGS. With this approach, we could indeed achieve recombination of RNA oligos. In a typical trial, the PUTT and REC reactions are each run at 42°C for 2 hr, and the products are then separated by 20% denaturing polyacrylamide gel electrophoresis. With the wild-type *Tetrahymena* L-21 ribozyme, we could detect 10% of the labeled **C•D** oligo being converted into **C•B** recombinant product when the 25-mer S-1t was used in PUTT and the 5′-radiolabeled 18-mer S-2t was used in REC (Figure 3, lane 1). The recombinant product **C•B** in this case is a 30-mer that cannot be the result of RNA degradation because it is larger than either of the two parental oligos.

We define recombination frequency as this 10% value,

Table 1. Oligoribonucleotides Used in This Study

RNA Oligo	Sequence	Length
S-1t	GGCCCUCU•AAAUAAAUAAAUAAAUA	25-mer
S-2t	GGAAAGGCCCUCU•AAAUA	18-mer
S-3t	GGCCCUCU•GGCCGAAACAGC	20-mer
S-4t	GGGACUCUGAUGAGGCCCUCU•AAAUA	26-mer
S-1a	GGCAU•AAAUAAAUAAAUAAAUA	22-mer
S-2a	GGAAAGGCAU•AAAUA	15-mer
S-3a	GGCAU•GGCCGAAACAGC	17-mer
S-3ad	GGCAU•GGCCAGUACAGC	17-mer
S-4a	GGGACUCUGAUGAGGCCCCAU•AAAUA	26-mer
S-hh	GGGCUGUC|AGUCC	13-mer

Oligoribonucleotides were purchased from Dharmacon (S-1t, S-2t, S-3t, S-1a, S-2a, S-3a, S-3ad, S-hh) or were prepared by run-off transcription from DNA templates (S-4t, S-4a). Suffix **t** indicates *Tetrahymena*; suffix **a** indicates *Azoarcus*; suffix **hh** indicates hammerhead. Underlined region is sequence complementary to the IGS region of group I ribozymes; dot (group I) or arrow (hammerhead) indicates expected cleavage site. All oligos are written 5′-head•tail-3′ (e.g., **A•B**).

semianalogous to the *RF* values that can be measured during meiotic events of eukaryotic chromosomes. However, note that in our RNA system, because we are only tracking one of two parental RNA oligos, *RF* values could theoretically approach 100%, while a maximum of 50% recombinant chromatids can be detected following meiosis.

To improve on this activity, we sought to minimize a competing side reaction, the hydrolysis of the acquired 3′ tail following the PUTT reaction. Mutations at a few positions in the catalytic core of the ribozyme have been shown to affect site-specific hydrolysis [22]. Consequently, we tested the ability of a particular mutant of the wild-type *Tetrahymena* molecule to catalyze recombination. A five-error mutant with base substitutions at positions 87, 103, 270, 271, and 312 was previously acquired through in vitro selection [23]. This mutant displays a greatly diminished rate of spontaneous tail hydrolysis, especially in buffers containing the divalent Ca^{2+} [24]. Even without Ca^{2+} in the buffer, when assayed for recombinase activity this mutant was in fact able to promote recombination to a greater extent. For the S-1t × S-2t cross in 50 mM $MgCl_2$, we routinely observed about 25% *RF* (Figure 3, lane 2). Consequently, we used this mutant in all subsequent recombination experiments with the *Tetrahymena* ribozyme. We were able to detect recombination in all crosses and reciprocal crosses among the oligos S-lt, S-2t, and S-3t, with *RF* values ranging from 6% to 25% (Table 2). In half of these cases of course, the expected recombinant product is not longer than both of the parents and thus cannot unambiguously be the consequence of recombination. Nevertheless, with a perfect match between expected and observed sizes of products, we can postulate that RNA-directed recombination with the *Tetrahymena* ribozyme is possible with a variety of oligonucleotide substrates.

The *RF* values for crosses and their respective reciprocal crosses are not the same within experimental error, despite the fact that we observe less than 12% variation in *RF* across replicate trials of a given cross (Table 2). A cross and its reciprocal are distinguished by which

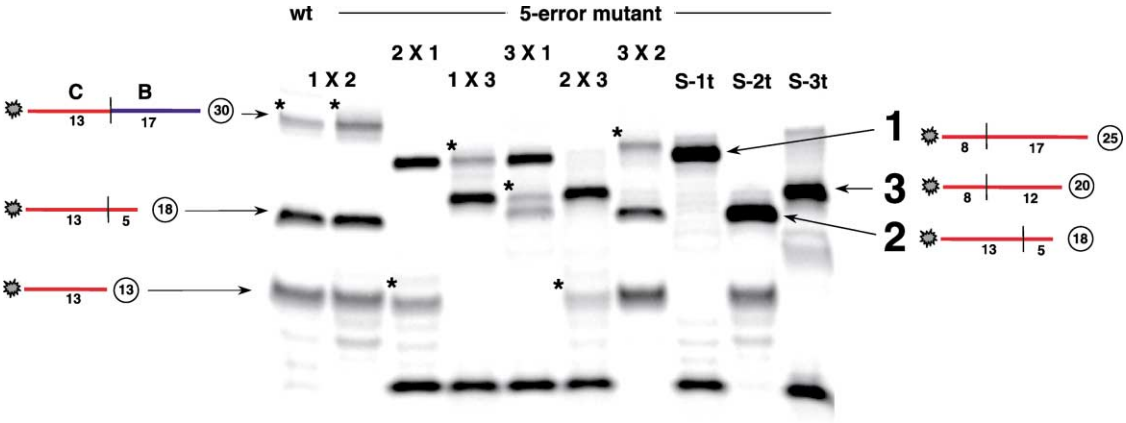

Figure 3. RNA Recombination Crosses and Reciprocal Crosses Catalyzed by the *Tetrahymena* Ribozyme with the Two-Pot Protocol

First lane, wild-type L-21 ribozyme; all other lanes, 5-error mutant L-21 ribozyme. In the first seven lanes, reactions **A•B** × **C•D** were performed as described in the main text, and products were run on a 20% denaturing polyacrylamide gel. **1**, S-1t; **2**, S-2t; **3**, S-3t. Only the second (**C•D**) oligonucleotide is 5′ radiolabeled, and thus the **A•B** oligos and their cleavage products are not visible on the gel. The diagrams on the left depict products for the S-1t × S-2t cross. In each case, recombinant products are bands denoted with asterisks in the upper left-hand corner. Occasionally, cleavage just adjacent to the canonical cleavage site can lead to an additional recombinant product (visible here for the S-3t × S-1t cross). In the last three lanes, control cleavage reactions were performed on **C•D** (no recombination).

Table 2. Recombination Frequencies of Oligonucleotide Substrate under Various Conditions

Ribozyme	Cross	Scheme	Salt Conditions	Reaction Time	*RF* *RF*(rc)
Tetrahymena (wild-type L-21)	S-1t × S-2t	two-pot	50 mM $MgCl_2$	2 hr (PUTT) +	11%
				2 hr. (REC)	10%
Tetrahymena (mutant)	S-1t × S-2t	two-pot	50 mM $MgCl_2$	2 hr (PUTT) +	25%
				2 hr. (REC)	16%
Tetrahymena (mutant)	S-1t × S-3t	two-pot	50 mM $MgCl_2$	2 hr (PUTT) +	21%
				2 hr (REC)	13%
Tetrahymena (mutant)	S-2t × S-3t	two-pot	50 mM $MgCl_2$	2 hr (PUTT) +	11%
				2 hr (REC)	6.3%
Tetrahymena (mutant)	S-1t × S-2t	one-pot	50 mM $MgCl_2$	4 hr	23% 16%
Tetrahymena (mutant)	S-1t × S-2t	one-pot	25 mM $MgCl_2$	4 hr	39% 15%
Tetrahymena (mutant)	S-1t × S-2t	one-pot	25 mM $MgCl_2$ + 10 mM $CaCl_2$	4 hr	31% 15%
Tetrahymena (mutant)	S-1t × S-3t	one-pot	50 mM $MgCl_2$	4 hr	20% 23%
Tetrahymena (mutant)	S-2t × S-3t	one-pot	50 mM $MgCl_2$	4 hr	12% 20%
Azoacrus	S-1a × S-2a	one-pot	50 mM $MgCl_2$	15 min	69% ND
Azoacrus	S-1a × S-2a	one-pot	25 mM $MgCl_2$	15 min	72% ND
Azoacrus	S-1a × S-2a	one-pot	25 mM $MgCl_2$ + 10 mM $CaCl_2$	15 min	78% ND
Azoacrus	S-1a × S-3a	one-pot	50 mM $MgCl_2$	15 min	46% ND
Azoacrus	S-3a × S-2a	one-pot	50 mM $MgCl_2$	15 min	34% ND
Azoacrus	S-3a × S-4a (hammerhead)	one-pot	25 mM $MgCl_2$ + 10 mM $CaCl_2$	1 hr	14% ND

RF values are the averages of 2–4 replicate trails; standard errors (s.d./$\sqrt{n}$) are 12% or less of average values in all cases. In each cross, the first oligo listed is **A•B**, input of 25 pmol; the second oligo listed is 5′ radiolabeled **C•D**, input of 1 pmol; in each case 10 pmol of ribozyme is used. *RF*(rc), *RF* values of the reciprocal cross; these values were not determined (ND) for *Azoarcus*.

substrate is used (unlabeled and in molar excess over the ribozyme) in the PUTT reaction and which is used (5′ labeled and in molar deficit with respect to the ribozyme) in the REC reaction. For example, the cross S-1t × *S-2t yields 25 ± 3% *RF*, while the reciprocal cross S-2t × *S-1t yields 16 ± 2% *RF*. This discrepancy is a consequence of the fact that different oligos must behave differently in the PUTT versus the REC reactions. With the S-1t, S-2t, and S-3t oligos, there is not enough variation to detect correlations between head or tail length and *RF*. Clearly, however, as is the case for larger 5′ and 3′ exons' rRNA transcripts [10], the sequence composition and potential base-pairing interactions both upstream and downstream of the splice site can affect the efficiencies of the splicing reactions.

One-Pot Recombination

For reactions that mimic the prebiotic scenario or for those to be involved in practical applications, recombination should proceed in a single milieu. We thus explored the ability of group I introns to catalyze recombination in a single reaction vessel containing the ribozyme and two (or more) substrates. For these assays, we incubated 10 pmol of ribozyme, 25 pmol of unlabeled **A•B** oligo, and 1 pmol of 5′-labeled **C•D** oligo in various buffers for 4 hr at 42°C. Under these conditions, we again observed significant recombination of all oligo pairs tested at *RF* values that typically met or even exceeded those for the two-pot scheme (Table 2). Thus, neither the physical separation of PUTT and REC steps nor the removal of spent **A** heads is necessary to achieve recombination. However, depletion of Mg^{2+} in the reaction buffer seems to promote recombination, such that the salt condition most favorable to recombination that we encountered was 25 mM $MgCl_2$. The *Tetrahymena* mutant used in these experiments is cleavage competent in Ca^{2+} alone [23], albeit at a catalytic efficiency 10^4-fold lower that in Mg^{2+}-containing buffers. We speculated that addition of Ca^{2+} to the reaction buffer could actually aid recombination by either retarding site-specific hydrolysis of tailed intermediates or by slightly remodeling the binding pocket to enhance displacement of the cleaved **A** heads by incoming **C•D** substrates. Addition of 10 mM Ca^{2+} to the reaction buffer slightly lowers the *RF* after 4 hr, but slows the kinetics of the reaction (see below) with the consequence that the *RF* peaks at about 2%–4% higher values than the 25 mM Mg^{2+} condition at later time points.

Because of the requirement for the second, or **C•D** oligo, to compete directly for binding to tailed ribozymes with spent **A** heads, recombination in a one-pot scheme should be favored at higher temperatures and/or with weaker IGS-substrate interactions. Consequently, we investigated the propensity of the *Azoarcus* group I intron to catalyze RNA recombination. The optimal temperature of this ribozyme is approximately 60°C, despite being isolated from a mesophilic bacterium having an optimal growth temperature of 42°C. Burke and colleagues had shown one instance in which a particular construct of this ribozyme could sequentially ligate exons from two different sources into polymers of heterogenous sequence and length and speculated that similar reactions should be able to promote recombination of prebiological relevance [18]. Their system utilized an externalized guide sequence of ten nucleotides and did not result in the recombination of heads and tails from different parental RNAs.

We constructed an *Azoarcus* ribozyme containing three nucleotides in its internal guide sequence and with a 3′ guanosine as a nucleophile (L-8 G204/G205; Figure 1B). We reasoned that this would allow more generalized recombination than possible with other systems. This 3-nt (GUG) IGS binds to and cleaves substrates possessing the trinucleotide CAU (and CAC to a lesser ex-

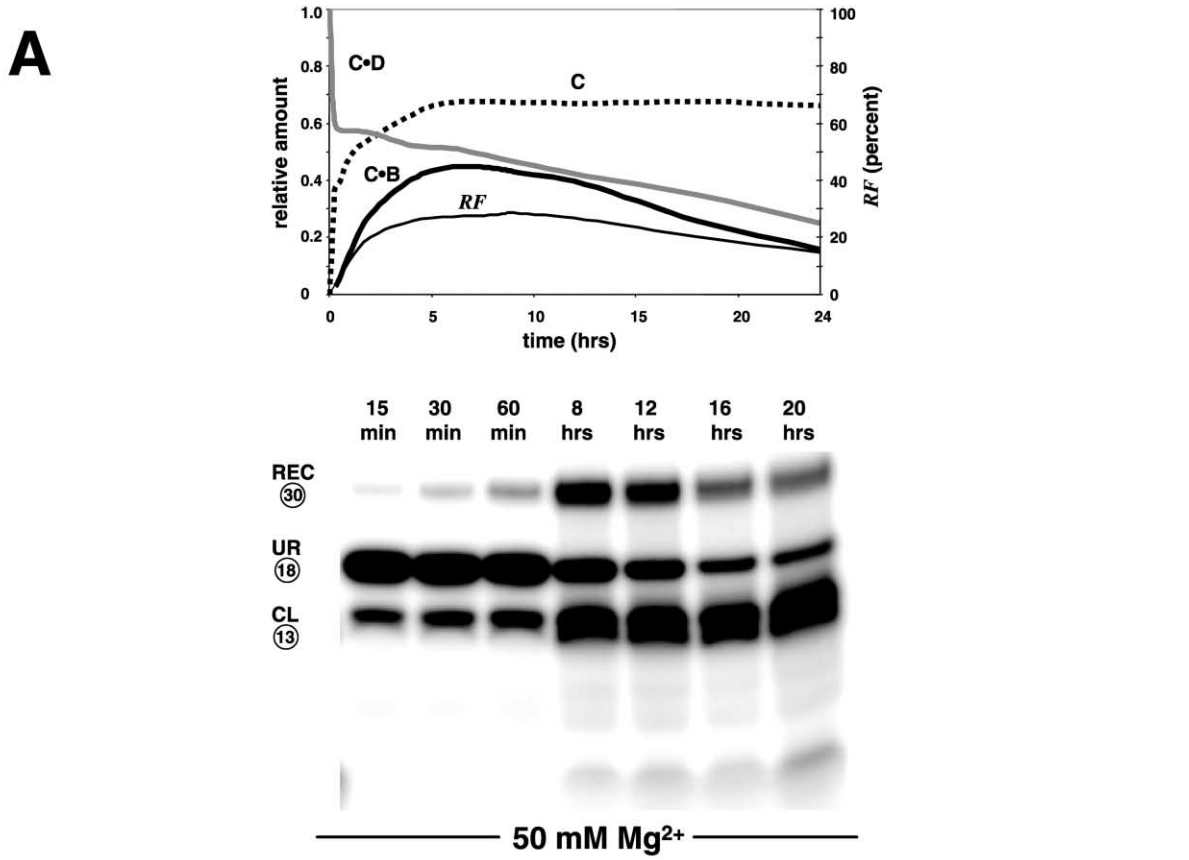
A
relative amount
RF (percent)
time (hrs)
C•D
C
C•B
RF
15 min
30 min
60 min
8 hrs
12 hrs
16 hrs
20 hrs
REC (30)
UR (18)
CL (13)
50 mM Mg2+
B
relative amount
RF (percent)
time (min)
C•D
RF
C•B
C
0 0.5 1 2 3 5 7.5 10 12 15 20 25 30 60 120
REC (27)
UR (15)
CL (10)
50 mM Mg2+
25 mM Mg2+ / 10 mM Ca 2+

tent) instead of 10-nt substrates or even 6-nt substrates in the cases of the *Tetrahymena* or the yeast group II intron. Thus, the sequence constraints on the parental oligos are limited to the possession of (a single) CAU and the avoidance of any secondary structures that block interaction with the IGS. For example, if the parental oligos form strong duplexes with themselves or each other, they may be precluded from being substrates.

Our experiments show that this *Azoarcus* ribozyme in fact generates *RF* values at 60°C with equivalent oligos (S-1a, S-2a, and S-3a; Table 1) that exceed those of the *Tetrahymena* mutant at 42°C (Figure 4; Table 2). The highest of these values we have detected is 78%, which can be observed for the S-1a × *S-2a cross after only 15 min of incubation. Here, the 25 mM $MgCl_2$ + 10 mM $CaCl_2$ reaction conditions were the most supportive of recombination, and the complete inactivity of the wild-type *Azoarcus* ribozyme in Ca^{2+} alone [25] supports the proposition that Ca^{2+} is favoring recombination by better positioning all the reactants and not by participating directly in catalysis. The *Azoarcus* is also operational in the two-pot scheme, but because the *RF* values there are half to two-thirds of the corresponding one-pot values, we chose not to fully explore the two-pot reaction with this ribozyme. In any event, the one-pot RNA recombination catalyzed by the *Azoarcus* ribozyme is the most rapid (in terms of time to generate recombinant progeny), productive (in terms of moles of recombinant product produced), and efficient (in terms of *RF*) that we have observed. Also, we checked the fidelity of recombination by gel purifying the recombinant 30-mer and 27-mer oligos from the S-1t,a × S-2t,a 1-pot crosses and confirmed their nucleotide sequences via digestion with T1, U2, Phy M, *B. cereus*, and CL-3 RNases (data not shown).

Kinetic Characterization

To begin to study the kinetic features of RNA-directed recombination, we followed the time course of reactants and products of both the *Tetrahymena*-driven and the *Azoarcus*-driven one-pot recombination protocols. We realized that the equilibrium given above in Equation 1 is dynamic, and the proportion of recombinants could fluctuate over time as a consequence of competing side reactions. Example kinetic traces of the S-1t × S-2t and S-1a × S-2a recombination reactions are shown in Figure 4. With both ribozymes, the appearance of the recombinant RNA oligonucleotide is transient. With the *Tetrahymena* variant driving the S-1t × S-2t cross using a 25:10:2::**A•B**: enzyme:**C•D** stoichiometry, the production of the recombinant peaks is at about 9 hr at an *RF* of 28% (Figure 4A). After this, the cleavage of both parental oligos and recombinant products, coupled with tail hydrolysis, results in a buildup of head and tail portions that are unable to participate in recombination. A similar phenomenon is observed with the *Azoarcus*-driven recombination of S-1a × S-2a. Here, however, the reaction reaches its peak much sooner. In 50 mM Mg^{2+}, the molar production of recombinant product is maximal after 20–25 min, while the *RF* peaks at about 1 hr (Figure 4B, left). The offset of these two peaks is a consequence of spontaneous RNA degradation under the reaction conditions (60°C, pH 7.5) that seem to affect the parental **C•D** oligo more severely than the recombinant **C•B** oligos, the latter having been more recently produced. The replacement of some Mg^{2+} divalent with Ca^{2+} retards both the peaks but delays the onset of spontaneous hydrolysis (Figure 4B, right). The degradation of the recombinant product is particularly slow in 25 mM Mg^{2+} + 10 mM Ca^{2+}; consequently, the apparent *RF* continues to rise.

The recombination of two oligos can be modeled as a coupled multistage system. In the first stage, the ribozyme must bind and cleave substrate **A•B**. In the second stage, the ribozyme must release **A**, bind **C•D**, and perform transesterification to generate the recombinant oligo **C•B**. In the third stage, the ribozyme either releases **C•B** or cleaves it to generate **C**. Because group I ribozymes are known to participate in sequential bind-and-release reactions with oligonucleotide substrates [9, 17], any uncleaved substrate can be recycled into the binding pocket of tailed ribozymes and participate in a transesterification; recombination itself requires such an event. Accordingly, a detailed kinetic description of this system is quite complex and will be published elsewhere. However, tracking of 5′ end-labeled **C** moieties, as in Figure 4, allows a simplified analysis of three particular states in the system by the following relationship:

$$\mathbf{C} \xleftarrow{k_{13}} \mathbf{C{\bullet}D} \underset{k_{21}}{\overset{k_{12}}{\rightleftarrows}} \mathbf{C{\bullet}B} \xrightarrow{k_{23}} \mathbf{C}. \qquad (2)$$

In addition, each of the three states can undergo spontaneous hydrolytic degradation ($k_{hyd,CD}$, $k_{hyd,CB}$, and $k_{hyd,C}$). We approximated the relative observed values of these rate constants for the purpose of qualitatively comparing the *Tetrahymena* and *Azoarcus* ribozymes, with the caveats that these rate constants subsume both the substrate binding and chemical catalysis phases of their respective transformations and that there are likely alternative reaction schemes such that the probability of a type II error is high. By fitting the above model to the data (e.g., Figure 4) for the 50 mM Mg^{2+} condition, we estimate for *Tetrahymena* the following values: $k_{12} \approx 0.1$ hr^{-1}, $k_{21} \approx 0.05$ hr^{-1}, $k_{23} \approx 0.01$ hr^{-1}, $k_{13} \approx 0.2$ hr^{-1}, $k_{hyd,CD} = k_{hyd,C} \approx 0.0001$ hr^{-1}, and $k_{hyd,CB} \approx 0.001$ hr^{-1}. Similarly, for *Azoarcus* we estimate the following values: $k_{12} \approx 0.04$ min^{-1}, $k_{21} \approx 0.02$ min^{-1}, $k_{23} \approx 0.005$ min^{-1}, $k_{13} \approx$

Figure 4. Recombination Kinetics

(A), single-pot recombination time course of the *Tetrahymena* ribozyme variant (S-1t × *S-2t); (B), single-pot recombination time course of the *Azoarcus* ribozyme (S-1a × *S-2a). Shown at the top of each panel are plots of the course of the reactions as quantified by phosphorimaging. The left axis (traces: gray, **C•D**, unreacted oligo; black, **C•B**, recombined; dashed, **C**, cleaved) is molar relative amounts standardized to unreacted at time zero = 1.0. The right axis (thin black trace) is recombination frequency: *RF* = [**C•B** /(**C•B** + **C•D** + **C**)] * 100%. Traces shown are based on averages from at least two independent time courses.

0.005 hr^{-1}, $k_{hyd,CD} \approx 0.02\ min^{-1}$, $k_{hyd,CB} \approx 0.01\ min^{-1}$, and $k_{hyd,C} \approx 0.03\ min^{-1}$. These values can be interpreted with respect to the predicted behaviors of the two ribozymes. First, as expected the catalysis of recombination (k_{12}) is faster for *Azoarcus*, roughly 24-fold. Second, both ribozymes appear to promote the forward recombination (k_{12}) twice as fast as the reverse (k_{21}), demonstrating that the stoichiometric bias of **A•B** over **C•D** is equally effective for both ribozymes. And third, the **C•D** → **C** cleavage side reaction (k_{13}) is much more of a problem for *Tetrahymena* than *Azoarcus*. This may be reflective of the temperature and IGS length differences; *Azoarcus* should be capable of more rapid exchange of substrate docked at the IGS such that recombination has a chance to take place prior to tail hydrolysis.

The production and transient nature of the recombinant oligos suggest that these group I ribozymes are capable of multiple turnover, such that they can function as true "recombinases." For recombination to occur, the ribozyme must sequentially bind and impart catalysis on two separate substrates, with an intervening release of one product (**A** heads). As noted above, the cleavage of recombinant **C•D** oligos into **C** and **D** portions requires that a third catalytic event be promoted by the group I ribozyme. Under stoichiometric conditions that are actually suboptimal for recombination, we can in fact observe the production of 1.2–1.4 *x* moles of product when *x* moles of *Azoarcus* ribozyme are allowed to recombine fresh substrates supplied in 20 min bursts (data not shown). Our inference is that individual ribozymes are not consumed in recombination and are free to recombine >1 pairs of oligonucleotides.

Construction of Functional Genetic Information via Recombination

To demonstrate one possible utility of recombination in an RNA world scenario, we endeavored to recombine two nonfunctional oligos into a functional one. As a target, we chose the hammerhead ribozyme motif. This catalytic RNA is small in size, approximately 35 nt, and it has been extensively characterized with respect to the nucleotides critical for function and its optimal reaction conditions [26, 27]. It contains a 5-nt loop that is relatively free of sequence constraints and is thus a logical site to insert an IGS sequence for RNA-driven recombination. We designed two RNA oligos, S-3a and S-4a (Table 1), which when recombined should create a full-length 33-nt hammerhead ribozyme. Each oligo contains roughly half the genetic information to create the hammerhead motif; each half makes a 5-bp helix with the 13-nt hammerhead substrate S-hh (Figure 5). However, the two halves also form a GC-rich 4-nt helix with each other, posing several secondary structure obstacles for one-pot recombination and subsequent hammerhead cleavage reactions. The *Azoarcus* ribozyme has characteristics that can alleviate some of these complications. First, the *Azoarcus* 3-nt IGS complement CAU can easily be engineered into the variable hammerhead loop but avoided in the remainder of the ribozyme and its substrate. Second, the optimum reaction temperature of the *Azoarcus* ribozyme is 60°C, a high enough temperature to destabilize premature base pairing between the S-3a, S-4a, and S-hh oligos. This optimal reaction temperature is sufficiently distinct from the hammerhead's (50°C) that the recombination and cleavage reactions can be partially thermally partitioned. And third, the *Azoarcus* and hammerhead ribozymes are both highly reactive under the same salt and pH conditions such that the 25 mM Mg^{2+}/10 mM Ca^{2+} (pH 7.5) combination most permissive of recombination should be effective.

Azoarcus-driven recombination of S-3a and S-4a can indeed create a functional hammerhead ribozyme that can cleave its substrate in a single reaction milieu (Figure 5). This is accomplished by a 30 min recombination at 60°C followed by a 2 hr incubation at 23° to 60°C. This two-phase thermal profile, accomplished uninterrupted in vitro in a PCR machine, is a reasonable mimic of diurnal cycling on the primitive Earth. Importantly, neither spurious interactions with the *Azoarcus* ribozyme alone, the noncovalently paired S-3a and S-4a oligonucleotides, nor the recombination of S-3a with a variant of S-4a (S-4ad, which creates three critical mutations in the catalytic core of the hammerhead, rendering it inactive) can promote site-specific cleavage of S-hh significantly above spontaneous background hydrolysis. However, the extent of hammerhead reaction is modest, as under these conditions we observe on average 2%, 6%, 10%, and 9% cleavage of S-hh at cleavage incubation temperatures of 23°C, 37°C, 50°C, and 60°C, respectively. Auspiciously, this relationship with temperature follows the temperature dependence of hammerhead ribozymes, which show peak activity at 50°C. When the S-hh substrate is not added until after the 30 min recombination period, we still observe 9% cleavage. In these reactions, the limiting factor is the competing stoichiometries of the two reactions. While a 25:1–2 ratio of **A•B** to **C•D** favors recombination, a large excess of either S-3a or S-4a over S-hh will shut down hammerhead cleavage via antisense base pairing. Conversely, an excess of S-hh over S-3a or S-4a inhibits recombination, which is relatively poor to begin with between S-3a and S-4a because of their partial complementarity. We have found that the ratio 1:2:2:1::S-3a:*Azoarcus*:S-4a:S-hh is the best compromise between all of these conflicts. In principle, other catalytic RNA motifs, including perhaps the recombinase ribozyme itself, can be similarly articulated via recombination of RNA oligonucleotides once the proper stoichiometric balance of reactants is achieved.

Significance

We have demonstrated the efficacy of RNA-directed recombination of RNA oligonucleotides. These data suggest that RNA recombination of oligonucleotides is facile with group I ribozymes. Here, we show that through recombination, one ribozyme can direct the synthesis of an entirely unrelated ribozyme. The recombination of larger RNAs should be feasible as well, such that entire catalytic RNA motifs could be built up from smaller RNAs through a series of energy-neutral reactions. Moreover, RNA recombinases were perhaps ancient feature of life. If true, then RNA recombination would be an important element in an RNA world scenario because recombination could help to coun-

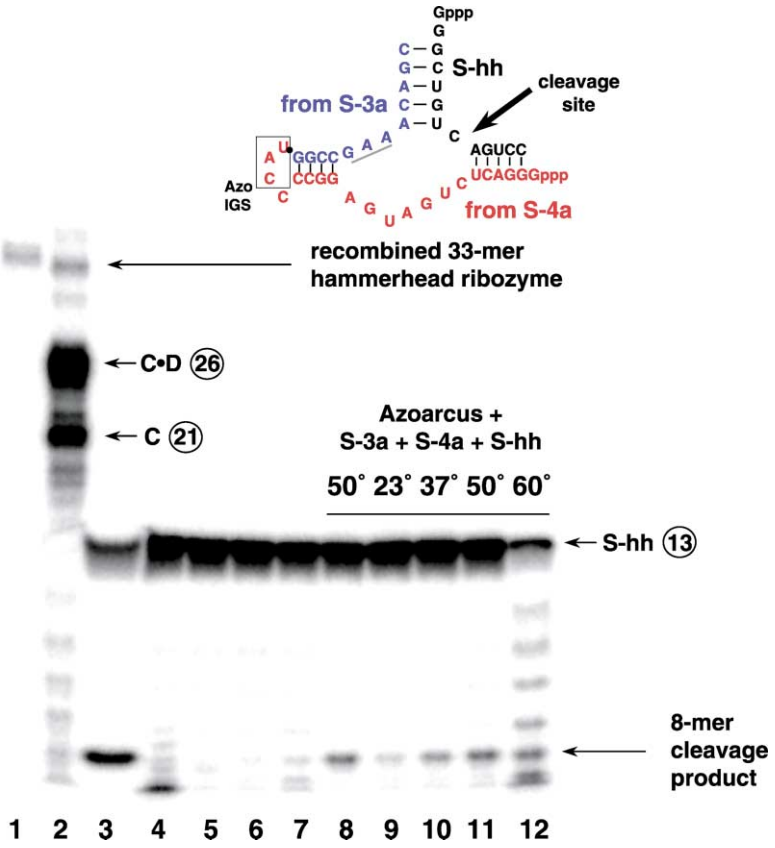

Figure 5. Construction of a Hammerhead Ribozyme via RNA-Directed Recombination

A scheme to construct the hammerhead ribozyme via RNA-directed recombination of RNA and allow hammerhead substrate cleavage is shown in color. The gel shows *Azoarcus*-driven recombination and reaction of hammerhead ribozyme in a single reaction vessel. Lane 1, 33-mer size control; lane 2, S-3a × S-4a recombination in the presence of S-hh (S-4a ^{32}P labeled); lane 3, positive control cleavage reaction using full-length hammerhead ribozyme (a run-off transcription from a DNA oligo, i.e., not from recombined RNA oligos) on 5′ ^{32}P-labeled S-hh. The S-hh 13-mer is cleaved into an 8-mer 5′ product (visible, indicated) and a 5-mer 3′ product (not visible). Lanes 4–12, cleavage products of 5 pmol of 5′ ^{32}P-labeled S-hh in 25 mM $MgCl_2$, 10 mM $CaCl_2$, 30 mM EPPS (pH 7.5) after 30 min at 60°C followed by 2 hr at 22–60°C, incubated with various other RNAs. Lane 4, incubated with 10 pmol *Azoarcus* ribozyme; lane 5, incubated with 5 pmol S-3ad, 10 pmol S-4a, and 10 pmol *Azoarcus* ribozyme with 2 hr incubations at 50°C. Oligo S-3ad contains three mutations (underlined in scheme: GAA → AGU) that render an inactive hammerhead ribozyme. Lane 6, incubated with 5 pmol S-3a and 10 pmol S-4a (no *Azoarcus*); lane 7, no added RNAs; lanes 8–12, incubated with 5 pmol S-3a, 10 pmol S-4a, and 10 pmol *Azoarcus* ribozyme with 2 hr incubations at indicated temperatures. For lane 8, S-hh was added after 30 min recombination (two-step protocol); for lanes 9–12, S-hh was present during recombination (uninterrupted protocol).

teract the degradation of genetic information through the accumulation of mildly deleterious mutations, a potentially severe problem with error-prone primordial RNA replicases [5]. Recombinase activity could have been an important supplementary functionality of early replicases; alternatively, primitive genomes may have acquired stand-alone recombinases whose modern-day descendants could include the group I and group II introns. RNA-directed recombination may also have practical applications today in the rapid in vitro construction of large RNA polymers.

Experimental Procedures

Materials

The *Tetrahymena* ribozymes were prepared as described earlier [23]. Briefly, plasmid pT7L-21 [28] was linearized with HindIII, and the ribozyme-encoding portion was subjected to mutagenesis. Mutant RNAs were obtained by run-off transcription and subjected to 12 rounds of in vitro selection for activity in 10 mM $CaCl_2$. The wild-type molecule and the 5-error mutant (at ribozyme positions 103, 187, 270, 271, and 312) were immortalized by cloning into pUC18. To prepare RNA for the current study, DNA from these plasmids was amplified with the following primers: primer A (5′–CTGCAG AATTCTAATACGACTCACTATAGGAGGGAAAAGTTATCAGGC–3′) and primer B (5′–CGAGTACTCCAAAACTAATC–3′), the latter ensuring that the 3′ end of the ribozyme contains an endogenous G nucleophile. RNA was generated from these plasmids via run-off transcription using T7 RNA polymerase (Ambion), purification by electrophoresis through 6% polyacrylamide/8M urea gels, and desalting of excised RNA from the gel through Nanosep MF and Nanosep 10K spin columns (Pall Gelman). The resulting RNA was rehydrated in 0.1 mM EDTA and quantified by UV spectrometry. The *Azoarcus* ribozyme [20] was obtained as a generous gift of Louis Kuo (Lewis and Clark College, Portland, OR) cloned into a pUC19 plasmid without 3′ guanosines at positions 204 and 205. These were restored in the molecule by PCR amplification using the primers TPM (5′–TAATACGACTCACTATAG–3′, which creates a promoter for T7 RNA polymerase) and T20a (5′–CCGGTTTGTGTGACTTTC GCC–3′, which adds G204 and G205). DNA oligonucleotides were purchased from Operon. RNA oligonucleotides were either purchased from Dharmacon or were obtained from run-off transcription of DNA oligos using T7 RNA polymerase (Ambion) and subsequently purified on 20% polyacyramide/8M urea gels. Salts and pH buffers were purchased from Sigma-Aldrich in the highest purity grade available. Urea, acrylamide (acrylamide:bis-acrylamide::19:1), and ribonucleotide triphosphates were purchased from Roche.

Recombination Assays

Two-pot recombination was achieved as follows. One RNA oligonucleotide (**C•D**) was 5′ end labeled using [γ^{32}P] or [γ^{33}P]•ATP (ICN) and T4 polynucleotide kinase (Roche), while the other oligonucleotide (**A•B**) was not labeled. For the PUTT reaction, typically 10 pmol of group I ribozyme (*Tetrahymena* or *Azoarcus*) was incubated with 25 pmol of **A•B** in a buffer containing 30 mM EPPS (pH 7.5) for 2 hr in a 10 μl volume. Reactions were carried out in various divalent metal ion conditions, such as 50 mM $MgCl_2$ or 25 mM $MgCl_2$ + 10 mM $CaCl_2$. Here, ribozymes were not thermally unfolded and refolded prior to reaction. *Tetrahymena* reactions were carried out at 42°C, while *Azoarcus* reactions were carried out at 60°C. After incubation, 50 mmol of EDTA was added to stop the reaction, and the volume was adjusted to 100 μl with H_20. The resulting solution was run through a Nanosep 30K spin column (Pall Gelman) at 5000 × g for 2.5 min. The retentate was adjusted to 10 μl total volume and heated to 80°C for 2 min. The appropriate buffer (includ-

ing divalent) was added, and the solution was cooled to room temperature. REC reactions were initiated by the addition of 2 pmol of 5′ end-labeled **C•D** substrate and incubated at the PUTT temperature for another 2 hr in a 20 μl volume. The resulting products were quenched with a solution containing 100 mM EDTA and gel loading solution (50% w/v urea, 0.5% sodium dodecyl sulfate, 10% sucrose, 0.01% bromphenyl blue) and loaded on 20% polyacrylamide/8M urea gels. Reaction products were visualized on a Typhoon (Molecular Dynamics) phosphorimager and quantified using ImageQuant software.

One-pot recombination was achieved similarly but in a single reaction vessel and without spin-column purification. In a typical reaction, 10 pmol of group I ribozyme was subjected to a heat/cool step in the appropriate reaction buffer. The recombination was initiated by the simultaneous addition of 25 pmol of unlabeled **A•B** substrate and 2 pmol of 5′ end-labeled **C•D** substrate in a 10 μl total volume. This mixture was incubated at 42°C (*Tetrahymena*) or 60°C (*Azoarcus*) for the appropriate length of time. The reaction was quenched with EDTA, and products were separated on 20% denaturing polyacrylamide gels and visualized by phosphorimaging.

RNA Oligonucleotide Sequencing

Crosses S-1t × S-2t and S-1a × S-2a were performed in a one-pot protocol employing 300 pmol ribozyme, 750 pmol S-1, and 100 pmol S-2 in 25 mM $MgCl_2$, 10 mM $CaCl_2$, 30 mM EPPS (pH 7.5) for 7 hr or 20 min, respectively. Products were separated by electrophoresis through 15% denaturing gels, and bands corresponding to the recombinant oligos were excised from the gel. RNA was eluted from the gel slices, purified by Nanosep 3K columns, and 5′ end labeled with γ^{32}P by T4 polynucleotide kinase (Roche). The kinased material was divided into six equal portions and treated with T1, U2, Phy M, *B. cereus*, and CL-3 RNases (Industrial Research, Lower Hutt, NZ) and carbonate buffer (pH 9, for alkaline hydrolysis ladder) for 5–15 min at 50°C [29]. The products were separated on a 20% denaturing polyacrylamide gel, and the resulting sequences of the recombination junction were confirmed by comparison to expectations.

Kinetic Assays

Kinetic assays were performed under the one-pot conditions as described above. The reactions were scaled up so that multiple equivalent aliquots could be taken. For example, to assay the S-1a × S-2a cross, 105 pmol of *Azoarcus* ribozyme was incubated with 260 pmol unlabeled **A•B** substrate and 10.5 pmol of 5′ end-labeled **C•D** substrate in a 105 μl total volume. After appropriate time points, ranging from 15 min to 24 hr in the case of *Tetrahymena* and 30 s to 2 hr in *Azoarcus*, 7 μl of the reaction mixture was quenched with EDTA and loaded onto 20% denaturing polyacrylamide gels. The fraction of each reaction that was either unreacted, reacted into recombinant product, or cleaved into 5′ heads was characterized by phosphorimaging. Rarely were any other product bands observed, except during longer incubations at 60°C, when hydrolytic degradation products were sometimes visible. The fractions of material present as unreacted (**C•D**), recombined (**C•B**), or cleaved (**C**) were plotted against time. The data were fit to a three-state model using the Poptools macro for Excel (http://www.cse.csiro.au/poptools/) to find approximate relative k_{obs} parameters that minimized deviation to the expected model. These values were used in simulations with Chemical Kinetics Simulator software (IBM) for general goodness-of-fit to observed traces. For turnover analysis, known molar amounts of *Azoarcus* ribozyme were incubated with S-1a and radiolabeled S-2a using a 10:4:6::**A•B**: ribozyme:**C•D** ratio in a one-pot format containing 25 mM $MgCl_2$ + 10 mM $CaCl_2$ for 20 min at 60°C. The resulting oligos were spun through a Nanosep 30K column and collected into 35 mM EDTA. Fresh S-1a and S-2a were added, a second 15 min reaction was performed, and the oliogonucleotide products were pooled with the first. This process was repeated ten times, and the pooled oligos were separated on a 20% denaturing polyacrylamide gel. The product bands, both **C•B** and **C**, were quantified by phosphorimaging, summed, and molar amounts were obtained by comparison to known concentration standards to determine by what fraction they exceeded the ribozyme amount used.

Hammerhead Recombination and Cleavage

To create by recombination and then react the hammerhead ribozyme in a single reaction vessel, substrates S-3a and S-4a were added to *Azoarcus* ribozyme in H_20, the mixture was heated to 80°C for 8 min, buffer was added, and the solution was cooled to room temperature. Then, 5′ end-labeled S-hh substrate was added to a total volume of 10 μl, and the mixture was brought to 60°C for 30 min and then back down to cleavage reaction temperature (23°C, 37°C, 50°C, or 60°C) for 2 hr in a PTC-200 thermalcycler (MJR). In separate reactions, the ratio of substrates to enzyme was varied to discover the optimum stoichiometry for cleavage. A typical reaction contained 5 pmol of S-3a, 10 pmol of S-4a, 10 pmol of *Azoarcus* ribozyme, and 5 pmol of S-hh. The buffer conditions were 30 mM EPPS (pH 7.5) with varying concentrations of divalent salts. A positive control reaction was performed in which the full-length hammerhead ribozyme (5′-pppGGGACUCUGAUGAGGCCCCAUGGCCGAA ACAGC-3′; IGS complement underlined) was obtained via run-off transcription from a DNA template, gel purified, and incubated with 5′ end-labeled S-hh under the same reaction conditions as the recombination trials. Negative controls included incubating the S-3a, S-4a, and S-hh oligos without *Azoarcus*, incubating the S-hh oligo with *Azoarcus* but without S-3a and S-4a, and performing the recombination exactly as described above but replacing S-3a with S-3ad, which creates a full-length but catalytically inactive hammerhead sequence. The products were separated on 20% denaturing polyacrylamide gels and visualized by phosphorimaging. The percentage of S-hh cleaved was calculated by dividing the intensity of the 8-mer product band by the sum of the intensity of the unreacted 13-mer band and the 8-mer product band, multiplying by 100%, and subtracting the equivalent value for a control lane in which all reactants were present but S-3a was replaced by S-3ad. The exception to this was the 2 hr incubation at 60°C, in which nonspecific hydrolysis of the S-hh substrate necessitated the use of the intensity of the unreacted 13-mer band from an adjacent lane to allow an accurate estimation of ribozyme-directed S-hh cleavage.

Acknowledgments

We thank D. Shub and L. Kuo for providing plasmid stocks of the wild-type *Azoarcus* ribozyme. We also appreciate technical assistance from D. Atkinson, A. Burton, A. Krummel, R. Madix, and W. Yu. This work was supported by grants from NASA (NAG5-11441) and NSF (DEB-0315286) to N.L. and by Portland State University.

Received: August 23, 2003
Revised: September 26, 2003
Accepted: September 30, 2003
Published: December 19, 2003

References

1. Kowalczykowski, S.C., Dixon, D.A., Eggleston, A.K., Lauder, S.D., and Rehrauer, W.M. (1994). Biochemistry of homologous recombination in *Escherichia coli*. Microbiol. Rev. *58*, 401–465.
2. Lai, M.M. (1992). RNA recombination in animal and plant viruses. Microbiol. Rev. *56*, 61–79.
3. Gilbert, W. (1986). The RNA world. Nature *319*, 618.
4. Cech, T.R. (1985). Self-splicing RNA: Implications for evolution. Int. Rev. Cytol. *93*, 3–22.
5. Lehman, N. (2003). A case for the extreme antiquity of recombination. J. Mol. Evol. *56*, 770–777.
6. Burke, D.H., and Willis, J.H. (1998). Recombination, RNA evolution, and bifunctional RNA molecules isolated through chimeric SELEX. RNA *4*, 1165–1175.
7. Biebricher, C.K., and Luce, R. (1992). *In vitro* recombination and terminal elongation of RNA by Qβ replicase. EMBO J. *11*, 5129–5135.
8. Kruger, K., Grabowski, P.J., Zaug, A.J., Sands, J., Gottschling, D.E., and Cech, T.R. (1982). Self-splicing RNA: autoexcision and autocylcization of the ribosomal RNA intervening sequence of Tetrahymena. Cell *31*, 147–157.
9. Zaug, A.J., and Cech, T.R. (1986). The intervening sequence RNA of *Tetrahymena* is an enzyme. Science *231*, 470–475.

10. Woodson, S.A., and Cech, T.R. (1989). Reverse self-splicing of the Tetrahymena group I intron: implications for the directionality of splicing and for intron transposition. Cell *57*, 335–345.
11. Sullenger, B.A., and Cech, T.R. (1994). Ribozyme-mediated repair of defective mRNA by targeted trans-splicing. Nature *371*, 619–622.
12. Lan, N., Howrey, R.P., Lee, S.W., Smith, C.A., and Sullenger, B.A. (1998). Ribozyme-mediated repair of sickle beta-globin mRNAs in erythrocyte precursors. Science *280*, 1593–1596.
13. Watanabe, T., and Sullenger, B.A. (2000). Induction of wild-type p53 activity in human cancer cells by ribozymes that repair mutant p53 transcripts. Proc. Natl. Acad. Sci. USA *97*, 8490–8494.
14. Bell, M.A., Johnson, A.K., and Testa, S.M. (2002). Ribozyme-catalyzed excision of targeted sequences from within RNAs. Biochemistry *41*, 15327–15333.
15. Welz, R., Bossmann, K., Klug, C., Schmidt, C., Fritz, H.-J., and Müller, S. (2003). Site-directed alteration of RNA sequence mediated by an engineered twin ribozyme. Angew. Chem. Int. Ed. Engl. *42*, 2424–2427.
16. Mörl, M., and Schmelzer, C. (1990). Group II intron RNA-catalyzed recombination of RNA *in vitro*. Nucleic Acids Res. *18*, 6545–6551.
17. Berzal-Herranz, A., Chowrira, B.M., Polensberg, J.F., and Burke, J.M. (1993). 2′-hydroxyl groups important for exon polymerization and reverse ligation reactions catalyzed by a group I ribozyme. Biochemistry *32*, 8981–8986.
18. Chowrira, B.M., Berzal-Herranz, A., and Burke, J.M. (1995). Novel system for analysis of group I splice site reactions based on functional *trans*-interaction of the P1/P10 reaction helix with the ribozyme's catalytic core. Nucleic Acids Res. *23*, 849–855.
19. Beaudry, A.A., and Joyce, G.F. (1992). Directed evolution of an RNA enzyme. Science *257*, 635–641.
20. Reinhold-Hurek, B., and Shub, D.A. (1992). Self-splicing introns in tRNA genes of widely divergent bacteria. Nature *357*, 173–176.
21. Kuo, L.K., Davidson, L.A., and Pico, S. (1999). Characterization of the *Azoarcus* ribozyme: tight binding to guanosine and substrate by an unusually small group I ribozyme. Biochim. Biophys. Acta *1489*, 281–292.
22. Legault, P., Herschlag, D., and Cech, T.R. (1992). Mutations at the guanosine-binding site of the *Tetrahymena* ribozyme also affect site-specific hydrolysis. Nucleic Acids Res. *20*, 6613–6619.
23. Lehman, N., and Joyce, G.F. (1993). Evolution *in vitro* of an RNA enzyme with altered metal dependence. Nature *361*, 182–185.
24. Lehman, N., and Joyce, G.F. (1993). *In vitro* evolution: Analysis of a lineage of ribozymes. Curr. Biol. *3*, 723–734.
25. Kuo, L., and Piccirrilli, J.A. (2001). Leaving group stabilization by metal ion coordination and hydrogen bond donation is an evolutionarily conserved feature of group I introns. Biochim. Biophys. Acta *1522*, 158–166.
26. Fedor, M.J., and Uhlenbeck, O.C. (1990). Substrate sequence effects on "hammerhead" RNA catalytic efficiency. Proc. Natl. Acad. Sci. USA *87*, 1668–1672.
27. Dahm, S.C., and Uhlenbeck, O.C. (1990). Role of divalent metal ions in the hammerhead RNA cleavage reaction. Biochemistry *30*, 9464–9469.
28. Zaug, A.J., Grosshans, C.A., and Cech, T.R. (1988). Sequence-specific endoribonuclease activity of the *Tetrahymena* ribozyme: enhanced cleavage of certain oligonucleotide substrates that form mismatched ribozyme-substrate complexes. Biochemistry *27*, 8924–8931.
29. Kuchino, Y., and Nishimura, S. (1989). Enzymatic RNA sequencing. Methods Enzymol. *180*, 154–163.
30. Cech, T.R., Damberger, S.H., and Gutell, R.R. (1994). Representation of the secondary and tertiary structure of group I introns. Nat. Struct. Biol. *1*, 273–280.